immunoblot analysis. **A,** representative immunoblot image of COX1. Actin was used as the internal loading control. **B,** Quantification of COX1 expression. The normalized intensities of COX1 obtained from three separate identical experiments are shown in the histogram. Error bars represent S.E. of each sets of three experiments. **C,** Nuclear translocation of GR was decreased by the knockdown of dynein IC2. PC12 cells were transfected for 24 h with control siRNA, NF1 (249) siRNA, both NF1 (249) and dynein IC2 siRNAs before treatment with NGF. After 48-h NGF treatment, cells were harvested, and the cytoplasmic and nuclear proteins were extracted. Both cytoplasmic and nuclear fractions were subjected to immunoblot analysis using anti-GR antibody. TCPε1 and Lamin B1 were used as markers of the cytoplasmic and nuclear fraction, respectively. Representative images of three reproducible experiments are shown. **D and E,** COX-1 expression is downregulated by dynein IC2 siRNA treatment. PC12 cells were transfected for 24 h with control siRNA, NF1 (249) siRNA, or both NF1 (249) and dynein IC siRNAs before treatment with NGF. After 48-h NGF treatment, COX-1 expression in the cells was analyzed by immunoblotting using anti-COX-1 antibody. **D,** Representative immunoblot images of COX1. Actin was used as the internal loading control. Representative images of three reproducible experiments are shown. **E,** Quantification of COX-1 expression. The normalized COX-1 intensities obtained from three separate identical experiments are shown in the histogram. Error bars represent S.E. of each set of three experiments. F, G, and H, COX-1 knockdown recovered the inhibition of neurite outgrowth in NF1-KD PC12 cells. PC12 cells were transfected for 24 h with control siRNA, NF1 (249) siRNA, both NF1 (249) and COX-1 (1023) siRNAs, or both NF1 (249) and COX-1 (2618) siRNAs before treatment with NGF. After 48-h NGF treatment, COX-1 expression in cells was analyzed by immunoblotting with anti-COX-1 antibody, and the neurite length were measured. **F,** Representative immunoblot images of COX-1. Actin was used as the internal loading control. **G,** Differential

interference contrast images of PC12 cells treated with control siRNA [**a**], NF1 (249) siRNA [**b**], NF1 (249) and COX-1 (1023) siRNAs [**c**], and NF1 (249) and COX-1 (2618) siRNAs [**d**]. **H,** Measurement of neurite length of PC12 cells treated with the siRNAs. The average of the total length of PC12 neurites are shown on the y-axis. The data are expressed as means and S.E. of three independent experiments. For each experiment, more than 50 cells were counted.

Table 1. Pathway-based characterization of up- and downregulated genes and proteins in PC12 cells identified with 2D-DIGE, iTRAQ, and DNA array analysis.

A. Upregulated pathways

rank	keymolnet pathway	score	score (*P*-value)	protein
1	Calcium signaling pathway	16.145	1.38×10^{-5}	**14-3-3**, **Annexin** , cadherin , **Crm1** , DGK , **Importin** , Kinesin , nAChR , **S100** , VILIP1 , **vinculin**
2	Transcriptional regulation by GR	14.298	4.96×10^{-5}	**14-3-3h** , ANXA1 , AP-1 , CGA , collagenase , CRF , GR , GRb , **HSP70** , IBAT , RGS2
3	Wnt signaling pathway	13.59	8.11×10^{-5}	b-TRCP , cadherin , **CRMP** , **MAP**, **MAP1B** , **tub** , Wnt
3	Granzyme signaling pathway	13.59	8.11×10^{-5}	**a2M** , COLIV , **HSP70** , **lamin** , Laminin , PI-9 , **tub**
5	MMP signaling pathway	13.127	1.12×10^{-4}	**a2M** , COLIV, Laminin , laminin5 , LRP , MMP , MMP-10 , MMP-13 , MMP-19 , MMP-3 , PAI-2
6	Intermediate filament signaling pathway	12.449	1.79×10^{-4}	**14-3-3** ,**14-3-3z** , **AP3-C** , **dynein** , **IF-II** , **K8** , Kinesin , **lamin** ,**laminA** , **laminC**, **tub**
7	inflammasome signaling pathway	11.866	2.68×10^{-4}	AIM2 , caspase-1 , inflammasome , IPAF , NALP1 , NALP3 , PI-9
8	CD44 signaling pathway	11.135	4.45×10^{-4}	COLIV , collagen, **ERMP** , **ezrin** , Laminin , MMP , **tub**
9	CYP family	10.729	5.89×10^{-4}	CYP3A , CYP3A4 , CYP3A43 , CYP3A5 , CYP3A7 , CYP4 , CYP4B1
10	LHR signaling pathway	10.609	6.40×10^{-4}	CGA , hCG , LH , LHR

B. Downregulated pathways

rank	keymolnet pathway	score	score (*P*-value)	protein
1	Serotonin signaling pathway	17.213	6.58×10^{-6}	5HT3R , 5HT5AR , 5HT5R , EPAC , Ga(q/11) , Ga(q/11)bg , nNOS , PKC , PLA2
2	CaSR signaling pathway	14.799	3.51×10^{-5}	Ga(q/11) , Ga(q/11)bg , **PI4K** , PKC , PMCA
3	AMPAR signaling pathway	14.213	5.27×10^{-5}	Actin , AKAP5 , Liprin-a , PKC , **Protein 4.1G** ,**tub**
4	Calcium signaling pathway	13.962	6.27×10^{-5}	Actin , CRT , Ga(q/11) , Ga(q/11)bg , **Kinesin** , P2X , PKCg , PMCA4 , troponin
5	GABA signaling pathway	13.363	9.49×10^{-5}	Actin , AKAP5 , GABAAR , GABAARg , GABAARg3 , GABAARq , GABAR , PKC
6	calpain signaling pathway	13.188	1.07×10^{-4}	Actin , calpain , calpain8 , integrin b, **NF-M** , PKC , PKCg , PMCA , TN-T , **tub**
7	HDAC signaling pathway	13.1	1.14×10^{-4}	Ets , HDAC , HDAC11 , **HSP90** , IV-HDAC
8	Melanopsin signaling pathway	11.955	2.52×10^{-4}	Ga(q/11) , Ga(q/11)bg , melanopsin
9	JAM family signaling pathway	11.769	2.87×10^{-4}	Actin , int-aL/b2 , int-aM/b2 , int-aX/b2 , int-b2
10	Guanylate cyclase(receptor type) signaling pathway	10.916	5.18×10^{-4}	CNGC , **HSP70** , **HSP90** , phospholamban , PMCA , **Tyr3MOX**

KeyMolnet software was used to determine statistically overrepresented pathway categories among the up-/downregulated molecules in NF1-KD PC12 cells. The list contained 263 upregulated genes/proteins (iTRAQ, 62 proteins; 2D-DIGE, 32 proteins; DNA array, 185 genes) and 239 downregulated genes/proteins (iTRAQ, 35 proteins; 2D-DIGE, 20 proteins; DNA array, 186 genes) (Fig. 2A,B, Table

S6). The top 10 KeyMolnet pathways showing a significant association with up/downregulated genes/proteins are listed with rank, KeyMolnet pathway, score, and *P* value of the score. Bold molecules were identified by proteome analysis.

Figure 1

A.

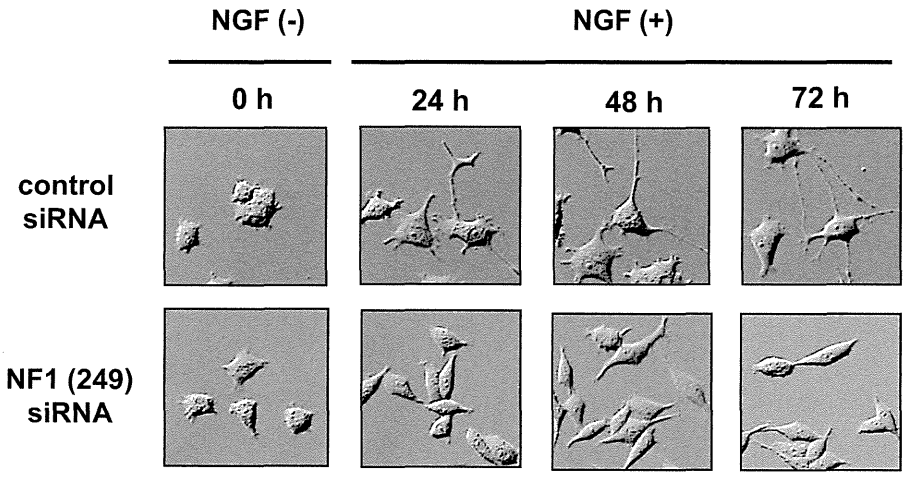
NGF (-)
NGF (+)
0 h
24 h
48 h
72 h
control siRNA
NF1 (249) siRNA

B.

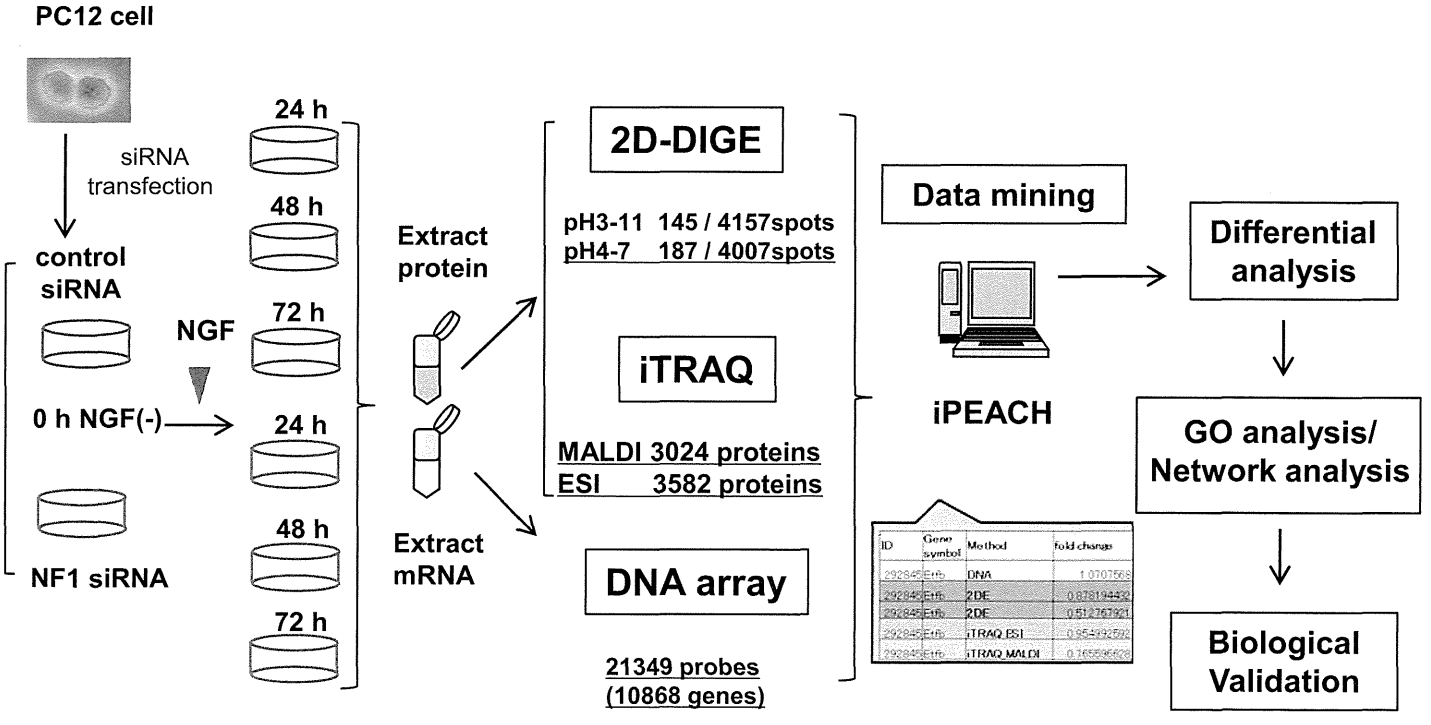
PC12 cell
siRNA transfection
control siRNA
NGF
0 h NGF(-)
NF1 siRNA
24 h
48 h
72 h
24 h
48 h
72 h
Extract protein
Extract mRNA
2D-DIGE
pH3-11 145 / 4157spots
pH4-7 187 / 4007spots
iTRAQ
MALDI 3024 proteins
ESI 3582 proteins
DNA array
21349 probes
(10868 genes)
Data mining
iPEACH
Differential analysis
GO analysis/ Network analysis
Biological Validation

Figure 2

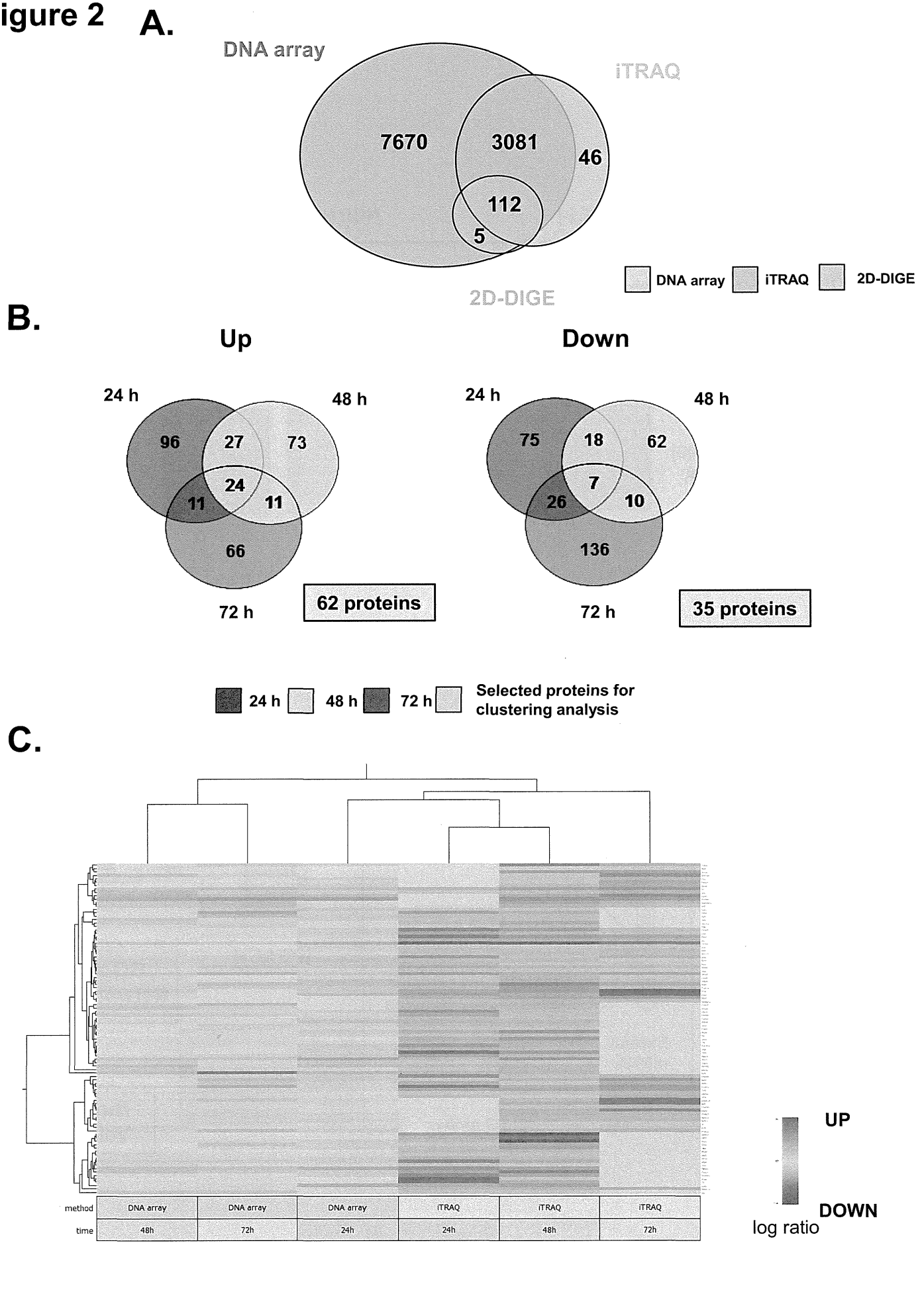
A.
DNA array
iTRAQ
2D-DIGE
7670
3081
46
112
5
DNA array
iTRAQ
2D-DIGE
B.
Up
Down
24 h
48 h
72 h
96
27
73
24
11
11
66
62 proteins
75
18
62
7
26
10
136
35 proteins
24 h
48 h
72 h
Selected proteins for clustering analysis
C.
method
time
DNA array
DNA array
DNA array
iTRAQ
iTRAQ
iTRAQ
48h
72h
24h
24h
48h
72h
UP
DOWN
log ratio

Figure 3

A.

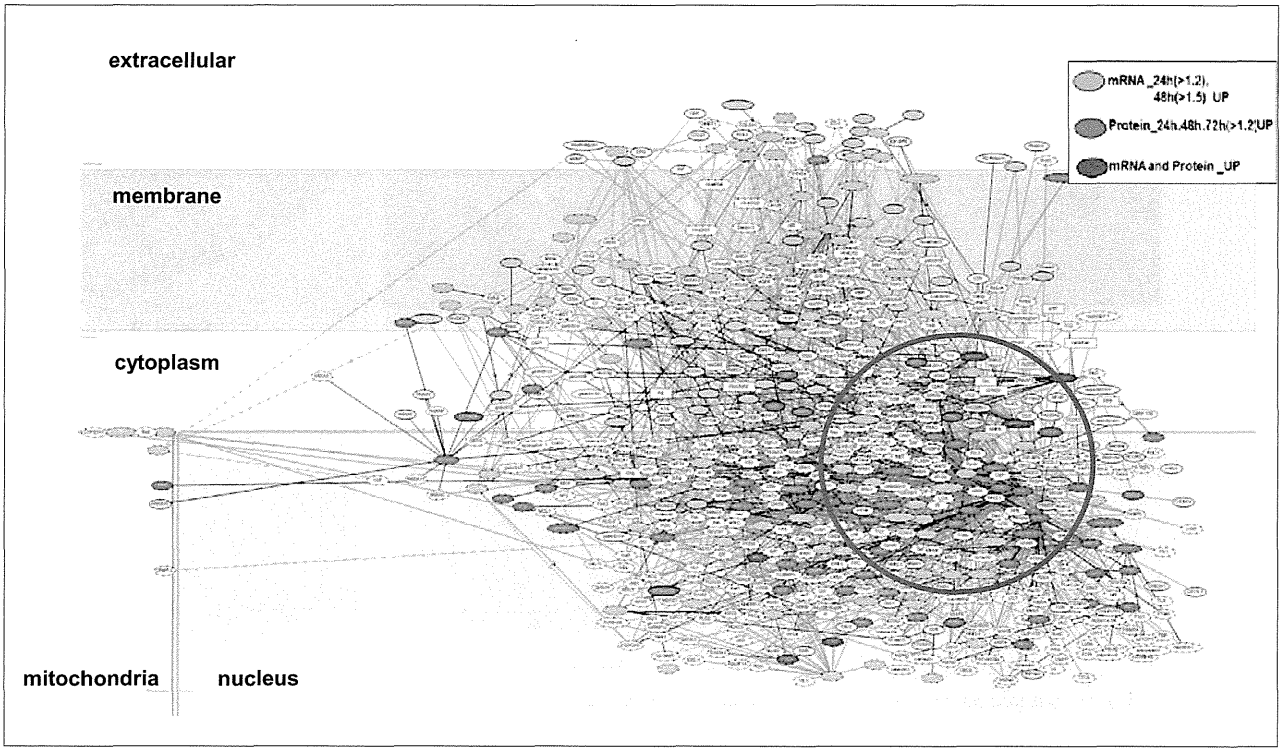
extracellular
membrane
cytoplasm
mitochondria
nucleus
mRNA_24h(>1.2), 48h(>1.5) UP
Protein_24h,48h,72h(>1.2)UP
mRNA and Protein _UP

B.

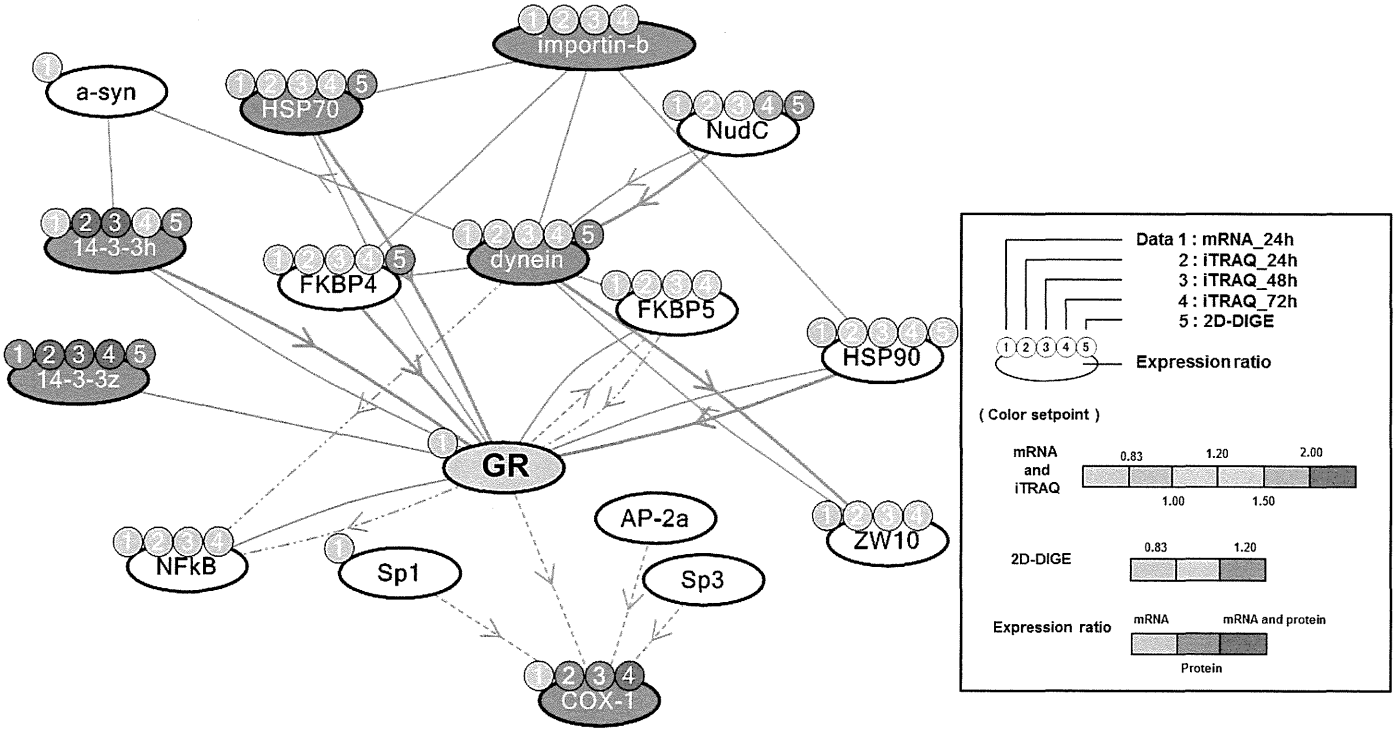
importin-b
a-syn
HSP70
NudC
14-3-3h
FKBP4
dynein
FKBP5
HSP90
14-3-3z
GR
AP-2a
ZW10
NFkB
Sp1
Sp3
COX-1
Data 1 : mRNA_24h
2 : iTRAQ_24h
3 : iTRAQ_48h
4 : iTRAQ_72h
5 : 2D-DIGE
Expression ratio
(Color setpoint)
mRNA and iTRAQ
0.83
1.20
2.00
1.00
1.50
2D-DIGE
0.83
1.20
Expression ratio
mRNA
mRNA and protein
Protein

Figure 4

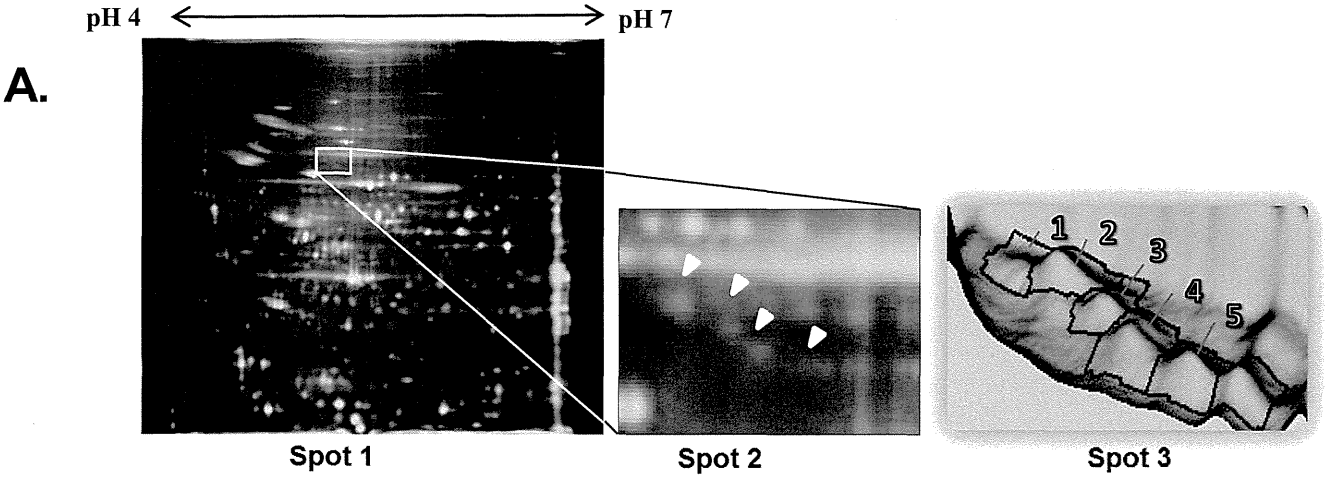
pH 4
pH 7
A.
1
2
3
4
5

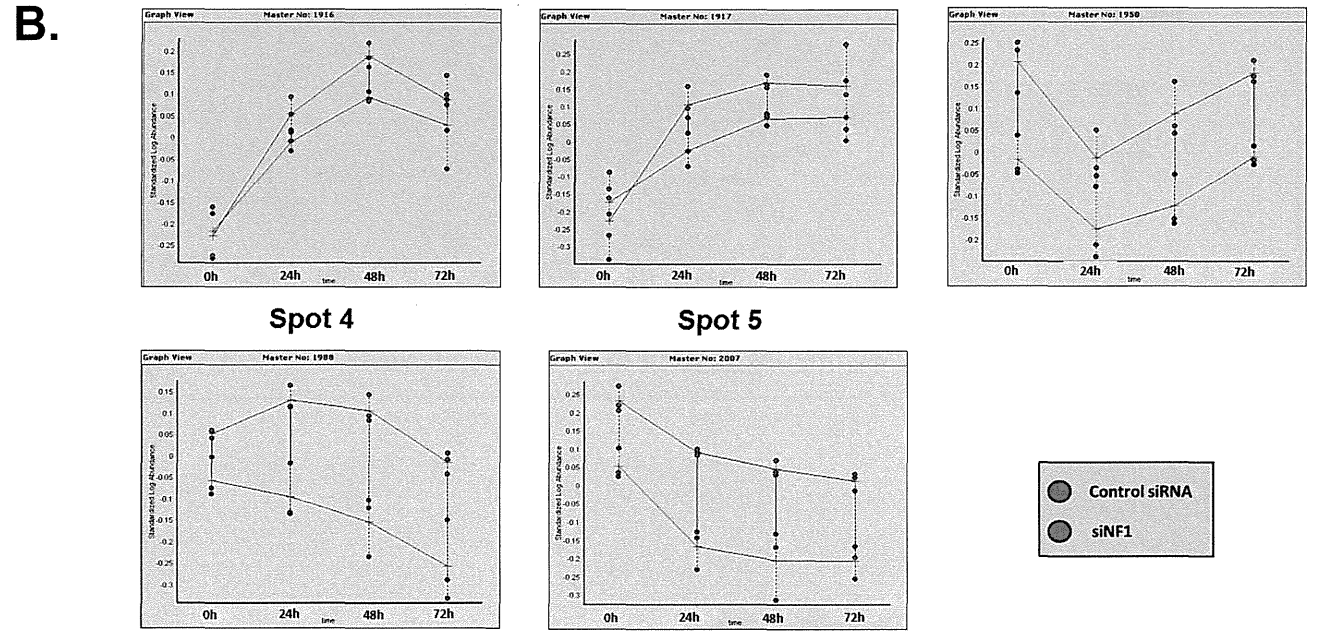
Spot 1
Spot 2
Spot 3
B.
Spot 4
Spot 5
0h
24h
48h
72h
Control siRNA
siNF1

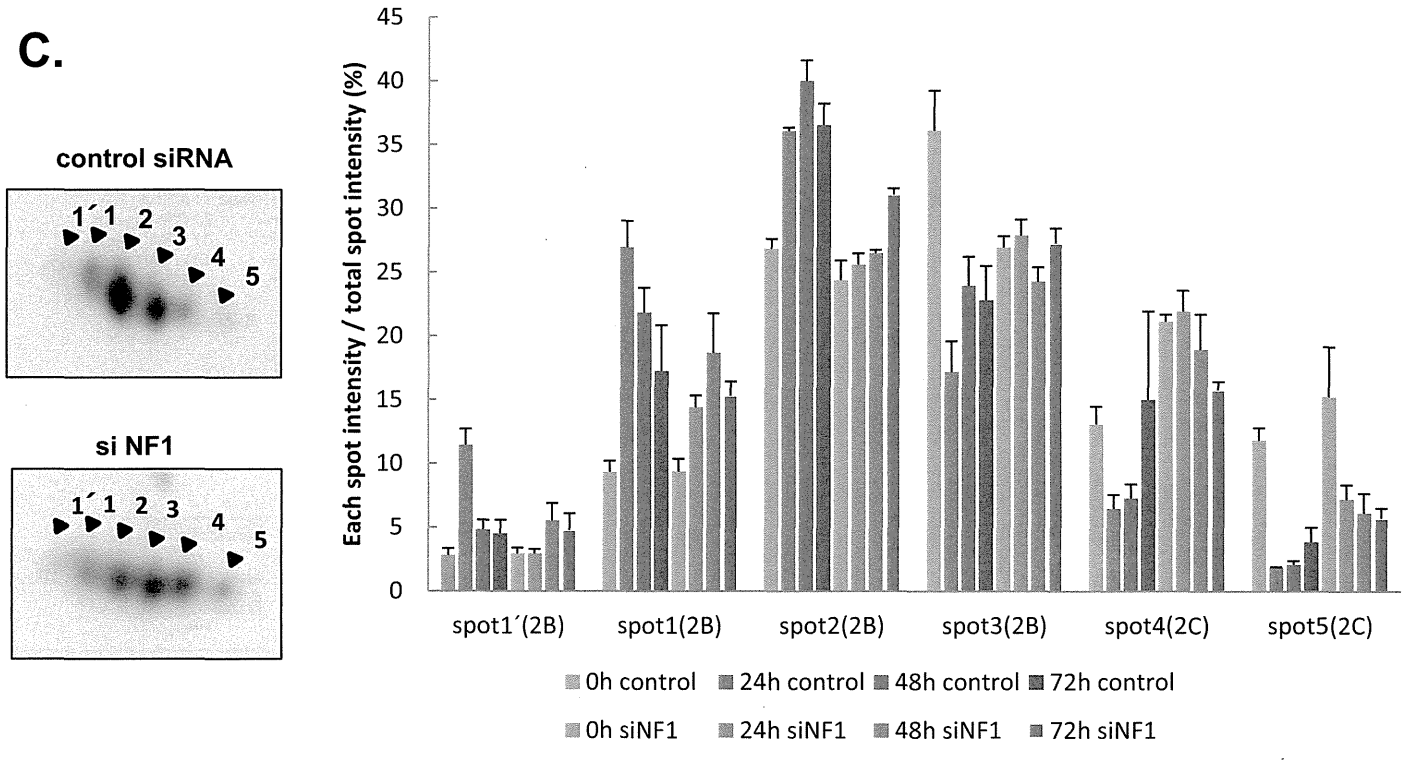
C.
control siRNA
si NF1
1´ 1 2 3 4 5
Each spot intensity / total spot intensity (%)
spot1´(2B)
spot1(2B)
spot2(2B)
spot3(2B)
spot4(2C)
spot5(2C)
0h control
24h control
48h control
72h control
0h siNF1
24h siNF1
48h siNF1
72h siNF1

Figure 4

D.

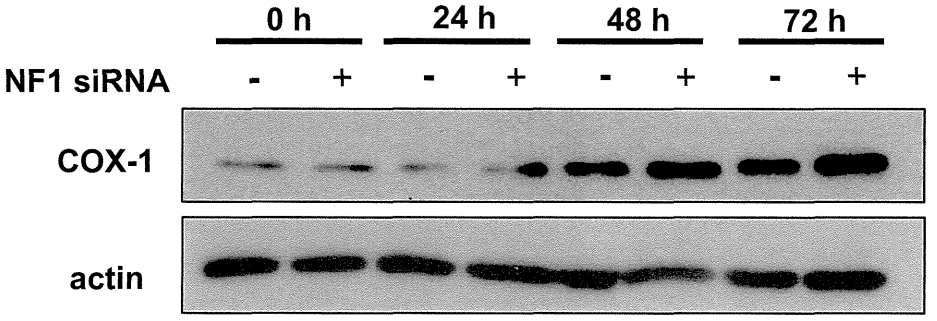
0 h
24 h
48 h
72 h
NF1 siRNA
- + - + - + - +
COX-1
actin

E.

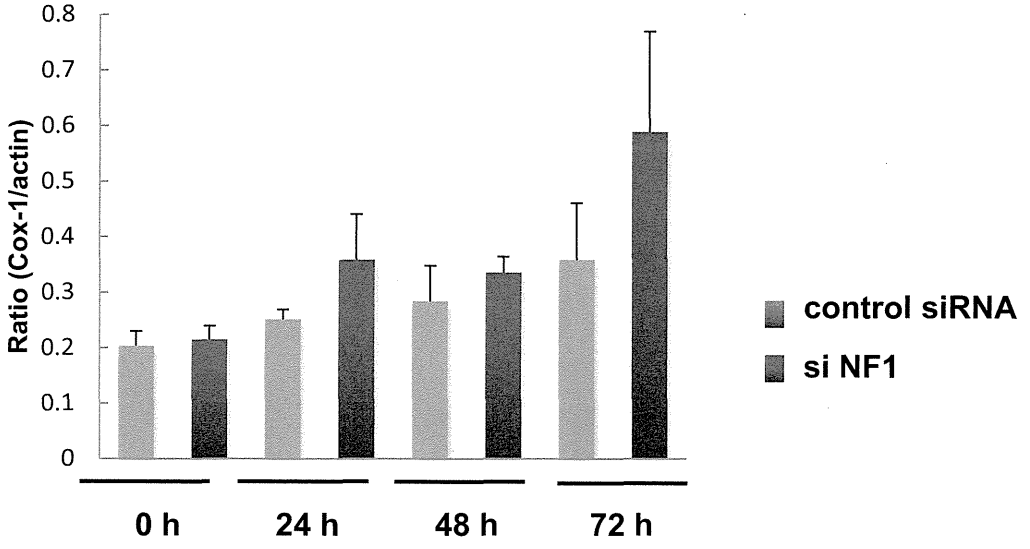
Ratio (Cox-1/actin)
0.8
0.7
0.6
0.5
0.4
0.3
0.2
0.1
0
0 h
24 h
48 h
72 h
control siRNA
si NF1

F.

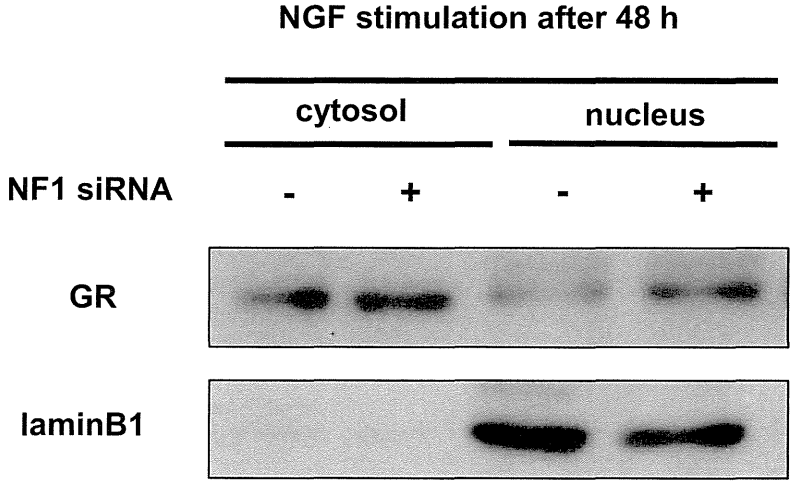
NGF stimulation after 48 h
cytosol
nucleus
NF1 siRNA
- + - +
GR
laminB1

Figure 5

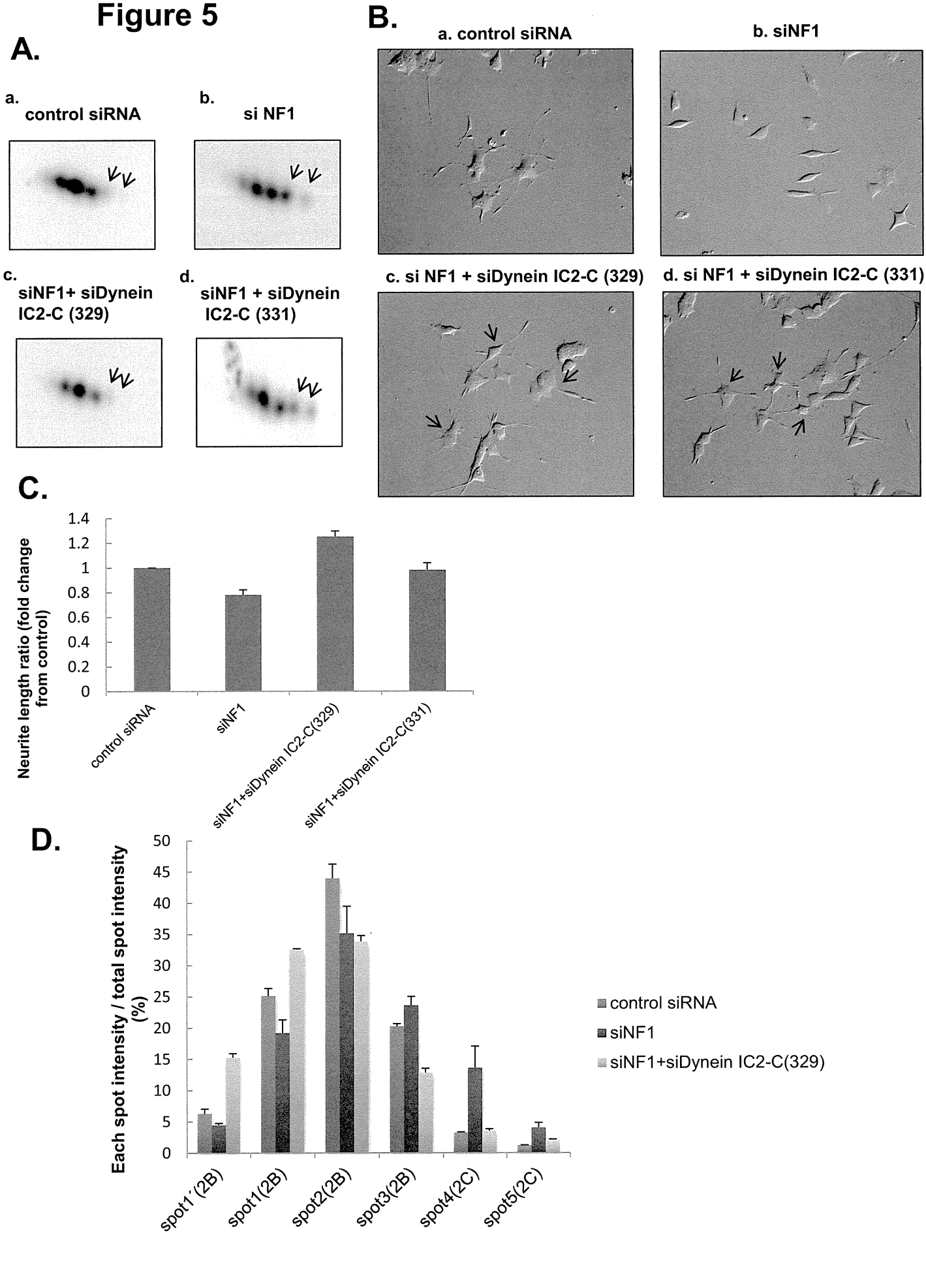
A.
a.
control siRNA
b.
si NF1
c.
siNF1+ siDynein IC2-C (329)
d.
siNF1 + siDynein IC2-C (331)
B.
a. control siRNA
b. siNF1
c. si NF1 + siDynein IC2-C (329)
d. si NF1 + siDynein IC2-C (331)
C.
Neurite length ratio (fold change from control)
1.4
1.2
1
0.8
0.6
0.4
0.2
0
control siRNA
siNF1
siNF1+siDynein IC2-C(329)
siNF1+siDynein IC2-C(331)
D.
Each spot intensity / total spot intensity (%)
50
45
40
35
30
25
20
15
10
5
0
spot1´(2B)
spot1(2B)
spot2(2B)
spot3(2B)
spot4(2C)
spot5(2C)
control siRNA
siNF1
siNF1+siDynein IC2-C(329)

Figure 6

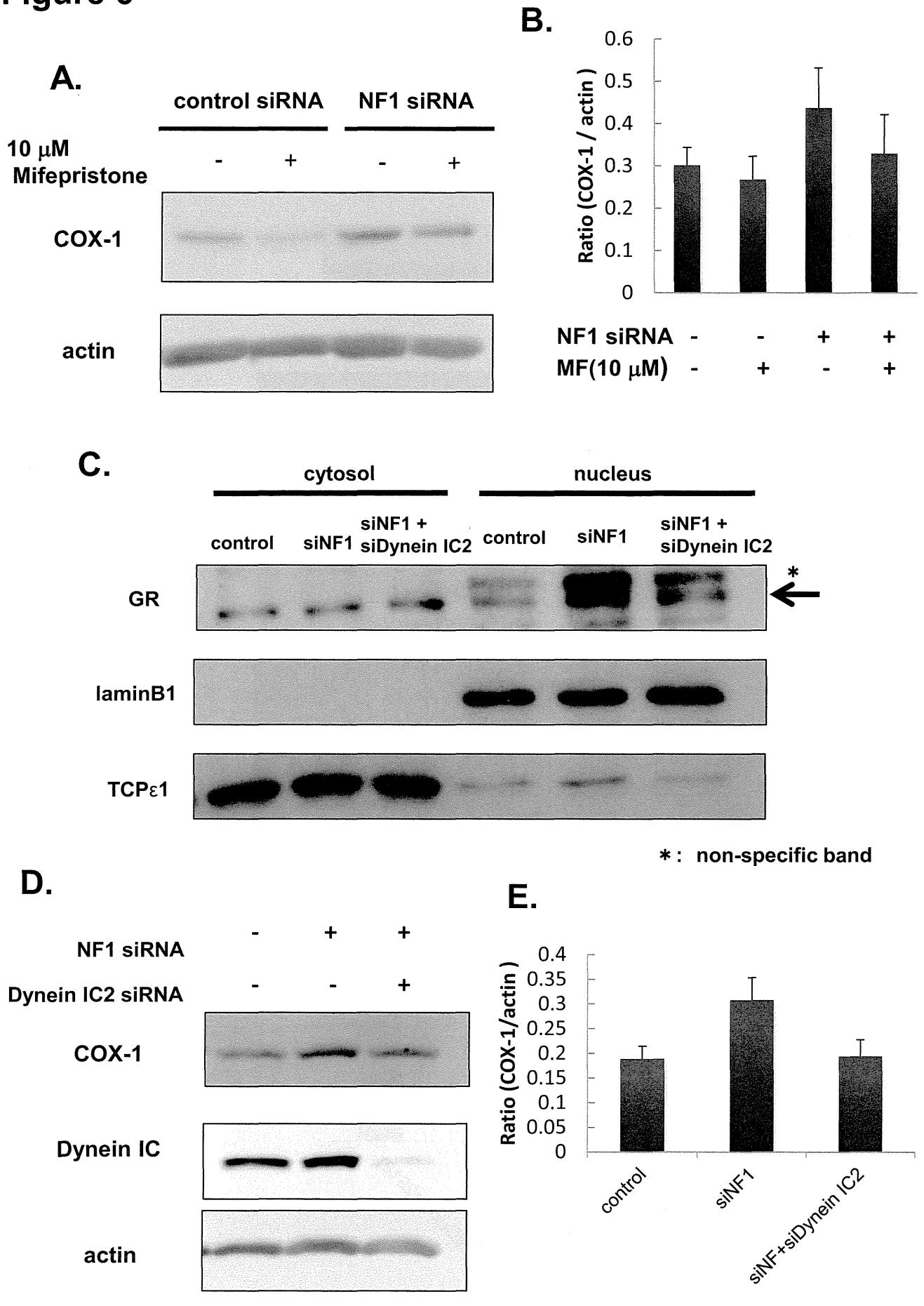
A.
control siRNA
NF1 siRNA
10 μM Mifepristone
- + - +
COX-1
actin
B.
Ratio (COX-1 / actin)
0.6
0.5
0.4
0.3
0.2
0.1
0
NF1 siRNA - - + +
MF(10 μM) - + - +
C.
cytosol
nucleus
control
siNF1
siNF1 + siDynein IC2
control
siNF1
siNF1 + siDynein IC2
GR
*
laminB1
TCPε1
* : non-specific band
D.
NF1 siRNA - + +
Dynein IC2 siRNA - - +
COX-1
Dynein IC
actin
E.
Ratio (COX-1/actin)
0.4
0.35
0.3
0.25
0.2
0.15
0.1
0.05
0
control
siNF1
siNF+siDynein IC2

Figure 6

F.

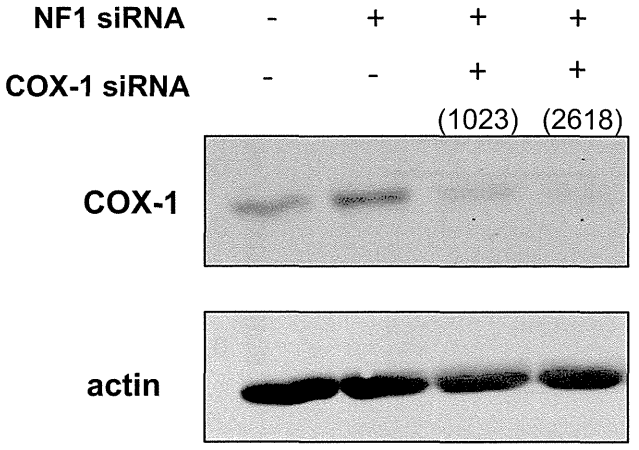
NF1 siRNA - + + +
COX-1 siRNA - - + +
(1023) (2618)
COX-1
actin

G.

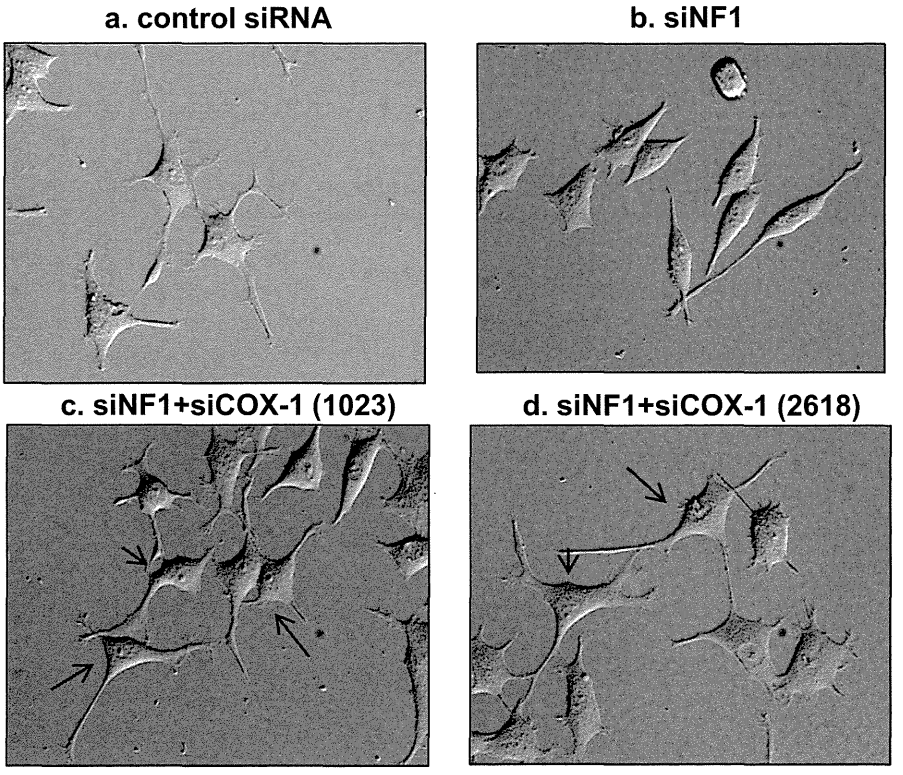
a. control siRNA
b. siNF1
c. siNF1+siCOX-1 (1023)
d. siNF1+siCOX-1 (2618)

H.

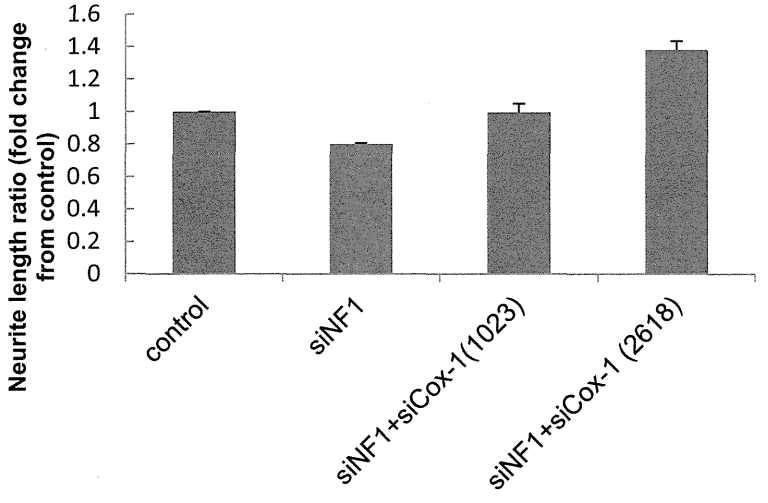
Neurite length ratio (fold change from control)
1.6
1.4
1.2
1
0.8
0.6
0.4
0.2
0
control
siNF1
siNF1+siCox-1(1023)
siNF1+siCox-1 (2618)

MCP Papers in Press. Published on January 28, 2013 as Manuscript M112.024802

Integrated proteomics identified novel activation of dynein IC2-GR-COX-1 signaling in NF1 disease model cells

Mio Hirayama[1]*, Daiki Kobayashi[1]*, Souhei Mizuguchi[1], Takashi Morikawa[1], Megumi Nagayama[1], Uichi Midorikawa[1], Masayo M. Wilson[1], Akiko N. Nambu[1], Akiyasu C. Yoshizawa[2], Shin Kawano[3], and Norie Araki[1**]

[1]Department of Tumor Genetics and Biology, Graduate school of Medical Sciences, Kumamoto University, 1-1-1, Honjo, Chuo-ku, Kumamoto 860-8556, Japan.

[2]Bioinformatics Center, Institute for Chemical Research, Kyoto University, Gokasho, Uji, Kyoto 611-0011, Japan

[3]Database Center for Life Science, Research Organization of Information and Systems, 2-11-16, Yayoi, Bunkyo-ku, Tokyo 113-0032, Japan

*These authors contributed equally to this work.

**To whom correspondence should be addressed: Norie Araki, Ph. D.

Department of Tumor Genetics and Biology, Graduate school of Medical Sciences,

Kumamoto University, 1-1-1, Honjo, Kumamoto 860-8556, Japan

Tel; +81-96-373-5119, Fax; +81-96-373-5210

E-mail; nori@gpo.kumamoto-u.ac.jp

Running Title: Integrated proteomics of NF1 disease model cells

Abbreviations

NF1-KD, NF1 knockdown; 2D-DIGE, two-dimensional fluorescence difference gel electrophoresis; iTRAQ, isobaric tagging for relative and absolute quantitation; iPEACH, Integrated Protein Expression Analysis Chart; NGF, nerve growth factor; GO, gene ontology; MANGO, Molecular Annotation by Gene Ontology; Qq-TOF, quadrupole/quadrupole/time-of-flight mass spectrometers; dynein IC, dynein intermediate chain; GR, glucocorticoid receptor; COX-1, cyclooxygenase-1; siRNA, short interfering RNA; MPNST, malignant peripheral nerve sheath tumor; PGE2, prostaglandin E2

Foot note

Authors' present addresses;

S Mizuguchi, Dept. Neurosurgery, Faculty of Medicine, University of Miyazaki, 5200 Kihara Kiyotake Miyazaki , 889-1692, Japan

T Morikawa, Mitsubishi Chemical Medience Corporation, 14, Sunayama, Kamisu, Ibaraki 314-0255, Japan.

U. Midorikawa, Healthcare Systems Laboratories, Sharp Corp. 1-9-2, Nakase, Mihama-ku, Chiba, 261-8520, JapanA. C. Yoshizawa, Koichi Tanaka Laboratory of Advanced Science and Technology, Shimadzu Corporation, Nishinokyo-Kuwabara-cho, Nakagyo-ku, Kyoto 604-8511, Japan

Summary

Neurofibromatosis type 1 (NF1) tumor suppressor gene product, neurofibromin, functions in part as a Ras-GAP, and though its loss is implicated in the neuronal abnormality of NF1 patients, its precise cellular function remains unclear. To study the molecular mechanism of NF1 pathogenesis, we prepared NF1 gene knockdown (KD) PC12 cells, as a NF1 disease model, and analyzed their molecular (gene and protein) expression profiles with a unique integrated proteomics approach, comprising iTRAQ, 2D-DIGE, and DNA microarrays, using an integrated protein/gene expression analysis chart (iPEACH). In NF1-KD PC12 cells showing abnormal neuronal differentiation after NGF treatment, of 3198 molecules quantitatively identified and listed in iPEACH, 97 molecules continuously up- or down-regulated over time were extracted. Pathway/network analysis further revealed overrepresentation of calcium signaling and transcriptional regulation by glucocorticoid receptor (GR) in the upregulated protein set, while nerve system development was overrepresented in the downregulated protein set. The novel upregulated network we discovered, "dynein IC2-GR-COX-1 signaling," was then examined in NF1-KD cells. Validation studies confirmed that NF1 knockdown induces altered splicing and phosphorylation patterns of dynein IC2 isomers, upregulation and accumulation of nuclear GR, and increased COX-1 expression in NGF-treated cells. Moreover, the neurite retraction phenotype observed in NF1-KD cells was significantly recovered by knockdown of the dynein IC2-C isoform and COX-1. In addition, dynein IC2 siRNA significantly inhibited nuclear translocation/accumulation of GR and upregulation of COX-1 expression. These results suggest that dynein IC2 upregulates GR nuclear translocation/accumulation, and subsequently causes increased COX-1 expression, in this NF1 disease model. Our integrated proteomics strategy, which combines multiple approaches, demonstrates that NF1-related neural abnormalities are, in part, caused by upregulation of dynein IC2-GR-COX-1

signaling, which may be a novel therapeutic target for NF1.

Introduction

Neurofibromatosis type 1 (NF1) is an autosomal dominantly inherited disorder with an estimated prevalence of 1 in 3,000 people (1). The hallmarks of NF1 include development of benign tumors of the peripheral nervous system and increased risk of malignancies. The phenotype of NF1 is highly variable, with several organ systems affected including the skin, bones, irises, and central and peripheral nervous systems. The effects on the nervous system are manifested in multiple neurofibroma, gliomas, and learning disabilities.

The NF1 gene is located on chromosome 17q11.2 and encodes a large protein of 2,818 amino acids, neurofibromin (2). Because the great majority of NF1 gene mutations frequently found in NF1 patients disturb the expression of intact neurofibromin, functional disruption of neurofibromin is potentially relevant to the expression of some or all of the abnormalities that occur in NF1 patients (3). A region centered around 360 amino acid residues encoded by the NF1 gene shows significant homology to the known catalytic domains of mammalian Ras GTPase-activating protein (p120 GAP). This region is also similar to yeast IRA1/2 proteins, which have been shown to interact with Ras and mediate hydrolysis of Ras-bound GTP to GDP, resulting in inactivation of Ras protein function. The GAP-related domain of the NF1 gene product also stimulates Ras GTPase and consequently inactivates Ras protein (4-6). In our previous report, we demonstrated a novel role of neurofibromin in neuronal differentiation in conjunction with regulation of Ras activity via its GAP-related domain using nerve growth factor (NGF)-stimulated PC12 cells as a model for neuronal cells (6). We also found that a novel neurofibromin interacting protein CRMP-2, identified with the screening of binding proteins of neurofibromin C-terminal domain by iTRAQ, upregulates the phosphorylation patterns in the NF1 siRNA treated PC12 cells compared with those of control cells through two-dimensional (2D) fluorescence difference gel

electrophoresis (DIGE) analysis coupled with Pro-Q Diamond staining, and demonstrated that the functional association of neurofibromin and CRMP-2 is essential for neuronal cell differentiation (7). In these studies, neurofibromin expression was suppressed using small interfering RNA (siRNA) directed against NF1, and the inhibition of neurofibromin functions caused neurite retraction via the regulation of Ras-MAPK-CDK5-GSK3/ROCK activation in differentiated PC12 cells stimulated by NGF (7). These results indicated that the neurofibromin-deficient PC12 cell is a useful model for analyzing NF1-related molecular pathology in detail.

Our previous research has examined specific genes and proteins related to phenotypic changes in neural tumors using integrated proteomic techniques such as 2D-DIGE combined with Pro-Q Diamond staining to identify phosphorylated proteins, isobaric tagging for relative and absolute quantitation (iTRAQ) (7, 8), which provides information on peptide/protein quantitative expression levels from different sources in a single experiment by liquid chromatography combined with tandem mass spectrometry (LC-MS/MS), as well as DNA array technology, utilizing the original data mining tool, MANGO (Molecular Annotation by Gene Ontology) (8). Processing the voluminous data arising from each analysis highlighted the need for a mining system for data integration. Therefore, we created the "iPEACH" (Integrated Protein Expression Analysis Chart, PCT/JP2011/58366) application to integrate information from several analysis types into a useful data file that provides comprehensive proteomic data including post-translational modification, transcriptomic data, and functional annotations from several databases, with a tool for quickly organizing, enriching, and sorting these data to reveal candidate molecules. Using iPEACH, sample data obtained from our transcriptomic and proteomic (iTRAQ and 2D-DIGE) analyses of NF1 disease model cells were integrated and stored in a database.

In this study, we constructed an iPEACH database for neurofibromin-deficient PC12 cells

compared with normal cells after NGF stimulation, and used Gene Ontology (GO) and knowledge-based network analyses targeting upregulated signals in the NF1 model cells, which lost their normal differentiation activity, to extract a novel candidate signal network for NF1-related phenotype, termed "dynein IC2-GR-COX1" signaling. Statistical analysis of the expression or modification of these proteins in NF1-knockdown (NF1-KD) cells and subsequent biological validation by sequential analyses using siRNAs and the glucocorticoid receptor (GR) antagonist led to the successful identification of protein targets of the network most likely to be involved in the abnormal PC12 differentiation caused by neurofibromin deficiency. In addition, this network involved the alternative splicing and specific phosphorylation of cytoplasmic dynein 1 intermediate chain 2 isoform B (dynein IC2-B) and isoform C (dynein IC2-C) via NGF stimulation in NF1-KD PC12 cells.

Here, we demonstrate that the function of neurofibromin for neurite outgrowth in PC12 cells may involve the regulation of cyclooxygenase-1 (COX-1) via glucocorticoid receptor (GR) and dynein IC2 splicing and phosphorylation. We also discuss the implications of a functional association between neurofibromin and COX-1 for neuronal regulation in relation to NF1 pathogenesis. This report is the first to identify a signal network related to NF1 phenotype in a neurofibromin-deficient neural model using our new integrated proteomics strategy.

Experimental procedures

Cell culture, NGF treatment, transfection, and preparation of cell lysate

PC12 cells were cultured under 5% CO_2 at 37°C in Dulbecco's modified Eagle's medium (Invitrogen)